Lasers in Medical Science (2019) 34:1555–1566
https://doi.org/10.1007/s10103-019-02741-4

ORIGINAL ARTICLE

Influence of radiant exposure and repetition rate in infrared neural stimulation with near-infrared lasers

Mohammad Javad Alemzadeh-Ansari[1] · Mohammad Ali Ansari[2] · Mahdi Zakeri[2] · Majid Haghjoo[3]

Received: 7 February 2017 / Accepted: 30 January 2019 / Published online: 18 March 2019

Abstract

In this study, we combine heat diffusion equation and modified Hodgkin-Huxley axonal model to investigate how an action potential is generated during infrared neural stimulation. The effects of temporal and spatial distribution of heat induced by infrared pulsed lasers on variation of electrical membrane capacitance are investigated. These variations can lead to depolarize the membrane and generate an action potential. We estimate the threshold values of laser light parameters such as energy density, pulse duration, and repetition rate are needed to trigger an action potential. In order to do it, we present an analytic solution to heat diffusion equation. Then, the analytic results are verified by experimental results. Furthermore, the modified Hodgkin-Huxley axonal model is applied to simulate the generation of action potential during infrared neural stimulation by taking into account the temperature dependence of electrical membrane capacitance. Results show that the threshold temperature increase induced by a train infrared pulse laser can be smaller if repetition rate is higher. These results also indicate that temperature rise time and axon diameter influence on threshold temperature increase. To verify threshold values estimated by the presented method, we use a train infrared pulsed laser ($\lambda = 1450$ nm with repetition rate of 3.8 Hz, pulse duration of 18 ms and energy density of 5 J/cm^2) to optically pace an adult rat heart, and we are able to successfully pace the rat heart during an open-heart surgery. The presented method can be used to estimate threshold values of laser parameters required for generating an action potential, and it can provide an insight to how the temperature changes lead to neural stimulation during INS.

Keywords Infrared neural stimulation · Axon · Heat diffusion equation · Optical pacing

Introduction

Infrared neural stimulation (INS) is an emerging method that can be applied to stimulate cochlea, vestibular system, peripheral motor nervous, and pacing embryonic and adult heart [1–8]. Jenkins et al. demonstrated that infrared stimulation can be used to pace adult heart. They evaluated the feasibility of optical pacing of an adult rabbit heart using a pulsed laser (1870 nm) with repetition rate 2.5 Hz, pulse width 8 ms, and energy density 6.3 J/cm^2. In this study, the heart was excised from a euthanized rabbit before cannulating and perfusing the heart on a modified Langendorff apparatus [9].

INS provides several advantages over conventional electric stimulation, including contact-free delivery, spatial precision, and lack of stimulation artifact [10, 11]. However, INS has limitations for neural prosthesis applications and damaging thermal effects of the stimulated beam. These limitations deal with heat deposition into tissue; reducing required optical energy while achieving neural stimulation is an important consideration [12]. The exact mechanism of INS is under discussion in the literature, but some results show that it is photothermal in nature [10–13]. Wells et al. have first demonstrated using pulsed infrared laser light to produce firing of an action potential through a thermal effect [8, 12–14]. Recent

Electronic supplementary material The online version of this article (https://doi.org/10.1007/s10103-019-02741-4) contains supplementary material, which is available to authorized users.

✉ Mohammad Ali Ansari
m_ansari@sbu.ac.ir

[1] Cardiovascular Intervention Research Center, Rajaie Cardiovascular Medical and Research Center, Iran University of Medical Sciences, Tehran, Iran

[2] Optical Bio Imaging Laboratory (OBI lab), Laser and Plasma Research Institute, Shahid Beheshti University, Velenjak, Tehran, Iran

[3] Cardiac Electrophysiology Research Center, Rajaie Cardiovascular Medical and Research Center, Iran University of Medical Sciences, Tehran, Iran

studies show that a rapid increase in temperature has an important role in neural stimulation during INS [2, 11, 14].

The generation and propagation of an action potential can be described by classical Hodgkin-Hulxey (HH) model that represents the biophysical properties of membrane by a conductance-based model. The lipid bilayer is modeled by a capacitance. In HH model, capacitance of the membrane is assumed to be constant but recent results show that a rapid increase in temperature can alter the electrical capacitance of plasma membrane and depolarization of target cell, and they show that the variation of electrical membrane capacitance is fully reversible [11]. This temperature dependency of membrane capacitance causes an extra membrane capacitor current that affects extracellular potentials. The classical HH model can be modified by taking into account capacitance-temperature relationship. This modified Hodgkin-Huxley axonal (MHHA) model can predict the threshold increase in temperature for generating action potentials. Fribance et al. applied MHHA model, and they illustrated that a rapid increase in local temperature produce a rapid increase in membrane capacitance, which results in an inward membrane current across the membrane capacitor strong enough to depolarize the membrane and generate an action potential [2].

Due to the difficulty of measuring thermal aspects of INS in vivo, numerical simulation was presented to simulate the thermal diffusion in neural phantoms. Monte Carlo and finite element methods were used by Thomson et al. and Norton et al. to determine heat distribution [15–18]. But, these attempts do not provide significant insight into how these temperature changes result in neural stimulation [12]. Norton et al. presented a complicated analytic framework describing time evolution of heat distribution induced by a single pulse laser and extracted thermal criteria for neural activation in special cases, where their results depicted that temporal evolution during INS depends on repetition rate and pulse duration of a train infrared pulsed laser [12, 19].

Based on results presented by Wells et al. and Shapiro et al., the mechanism of INS can be studied by photothermal mechanism [11–13]. In this approach, the effects of radiant exposure and repetition rate of infrared laser on temporal and spatial distribution of heat inside neural tissue is a critical issue. Here, we combine heat diffusion equation and MHHA model to simulate generation of an action potential during INS. The effect of laser light parameter such as energy density, pulse duration, and repetition rate on temperature variation is studied by heat diffusion equation. The threshold increase in temperature to generate an action potential is estimated by MHHA model. Hence, using presented method, we can estimate the threshold value of laser light parameter for generating an action potential inside a typical neural tissue. To verify these estimations, we conduct phantom and animal studies. The analytical results obtained by heat diffusion equation evaluate by phantom study. We estimate the threshold values of laser light parameters needed to optically pace an adult rat heart, and finally, we evaluate these values during an open-heart rat surgery.

Materials and methods

In this study, MHHA model is applied to explain generation of action potential during INS. To demonstrate this subject, we calculate the deposited thermal energy in neural tissues. We use the heat diffusion equation to simulate temporal and spatial temperature distribution during INS. The calculated maximal local temperature is applied to study changes in membrane capacitance, which results in in-ward membrane ionic current crossing the membrane capacitance. Hence, at first, we explain an analytic method to solve heat equation, and then we state the details of MHHA model to simulate generation of action potentials. At the end of this section, we explain details of experimental set up to evaluate this analytic method. Finally, we report the open-heart rat surgery to in situ optical pacing of an adult rat by INS.

Analytic method

The heat diffusion equation can be used to determine heat distribution [20]:

$$\frac{\partial T}{\partial t} = D\nabla^2 T(r,z,t) + \frac{1}{\rho C_P} S(r,z,t), \tag{1}$$

where T is temperature, t is time, r and z are spatial coordinate transverse and longitudinal to light propagation, respectively (see Fig. 1). D is heat conductivity, ρ is tissue density, and C_P is specific heat capacity. Herein, the S refers to heat source induced by absorption of laser radiation. The absorbed energy of laser depends on absorption coefficient of tissue α. The laser light exiting fiber core is described as a Gaussian divergent beam propagating through biological tissue:

$$S(r,z,t) = \frac{2\alpha E_0}{\pi a^2} \exp\left(-\frac{2r^2}{a^2}\right) \exp(-\alpha z) f(t), \tag{2}$$

That a describes the Gaussian beam, and $f(t)$ indicates the temporal shape of laser beam. We apply an appropriate green function

$$G\left(r-r', z-z', t-t'\right) = \frac{1}{[4\pi(t-t')]^{\frac{3}{2}}} \exp\left(-\frac{(r-r')^2 + (z-z')^2}{4a^2(t-t')}\right), \tag{3}$$

Compute $T(r, z, t)$ as follows:

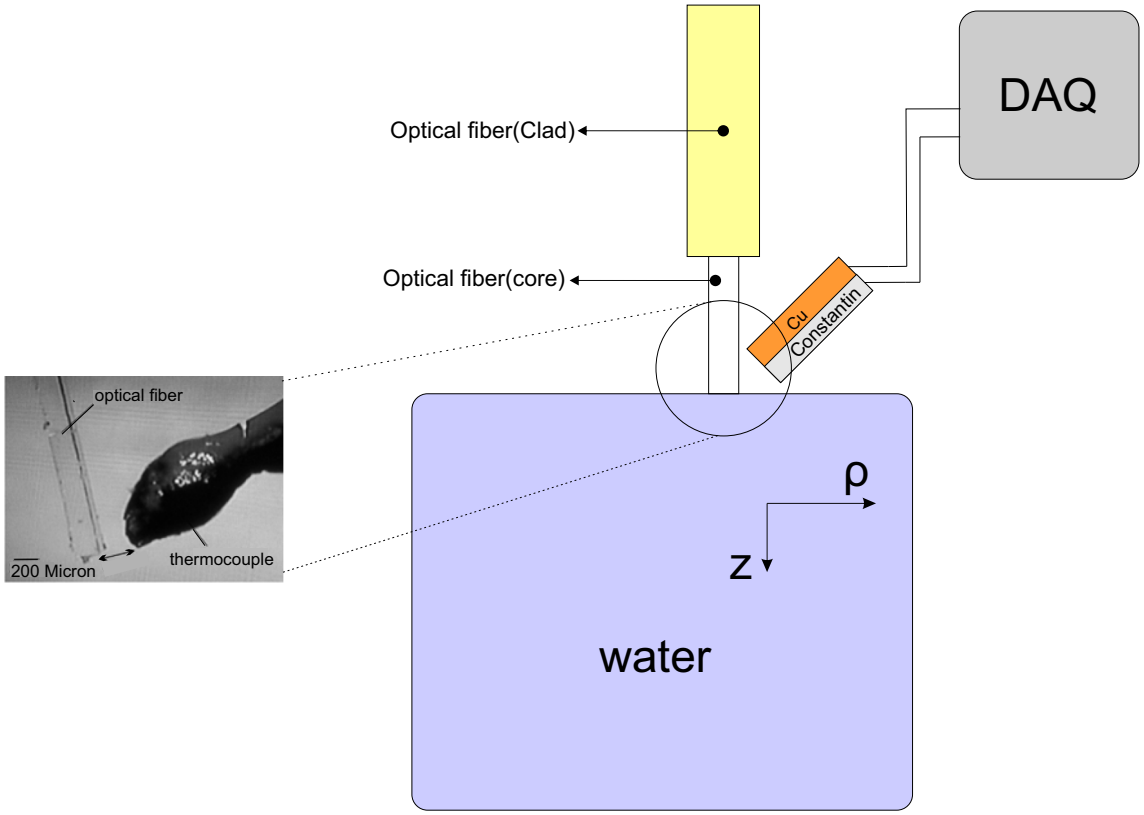

Fig. 1 Graphical representation of optical source and sample; the neural tissue lays a distance z axially from the optical fiber (right). The thermocouple is close to optical fiber core; the bar is 200 μm (Left)

$$T(r,z,t)=\frac{\alpha E_0\exp(-\alpha z)}{4\pi\rho C_P a^2}\int_0^t\frac{f(t')}{a^2+8D(t-t')}\exp\left(\frac{-2r^2}{a^2+8D(t-t')}\right)\exp\left(\alpha^2 D\left(t-t'\right)\right)\operatorname{ercf}\left(\frac{2\mathrm{D}\alpha(t-t')-z}{\sqrt{4D(t-t')}}\right)dt', \tag{4}$$

That ercf is the complementary error function defined as ercf(x) = 1 − erf(x). Equation 4 is a general solution to heat diffusion equation with no additional limitations or approximations that can be numerically computed. We use this equation to estimate the maximal temperature induced by absorption of laser during INS.

The MHHA model

In the classical HH model, capacitance of the membrane is assumed to be a constant parameter. It states that membrane capacitor current is described by a linear differential equation as follows:

$$I=c_m\left(\frac{dV_n}{dt}\right)+\sum_i I_i(t), \tag{5}$$

where c_m is membrane capacitance, V_n is the intracellular potential at nth segment (see Fig. 2), and $\sum_i I_i(t)$ depicts ionic currents. However, recent results show that the measured capacitance-temperature relationship can be fitted very well by following equation [2]:

$$c_m=c_0+\frac{k}{\Delta T}, \tag{6}$$

where c_0 is a constant membrane capacitance (0.824 μF/cm^2), k is a fixed parameter equals 2.2 μF.°C/cm^2, and ΔT is a change in temperature. One can modify the classical HH model by taking into account this capacitance-temperature relationship (we can add the term containing (dc_m/dt) into Eq. 5 as shown in Eq. 8).

The spatial-temporal distribution of the temperature along the axon induced by a Gaussian laser beam is described as follows [21]:

$$\begin{cases} T-T_0=\Delta T\exp\left(-\frac{2(r-r_l)^2}{a^2}\right)\frac{t}{t_r} & t\le t_r \\ T-T_0=\Delta T\exp\left(-\frac{2(r-r_l)^2}{a^2}-\frac{t-t_r}{T_d}\right) & t>t_r \end{cases}, \tag{7}$$

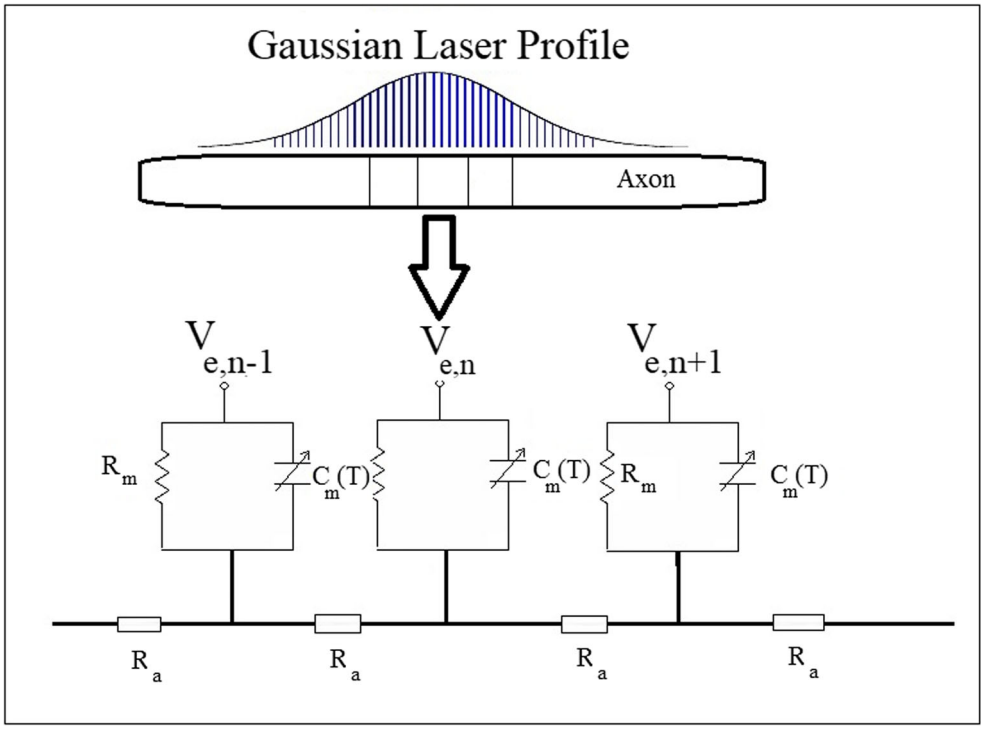

Fig. 2 Schematic of unmyelinated axon model to simulate generation of action potential by infrared pulsed laser. The axon is irradiated by a Gaussian laser beam. The unmyelinated axon is segmented into many rods with length Δx, and each of this rod is modeled by HH model. $V_{e,n}$ is the intracellular potential at n^{th} segment, $C_m(T)$ is temperature-dependent membarane capacitance, $R_m$is membrane resistance, and R_a is axoplasm resistance. The length is 9 mm

where T_0 is the global axon temperature, and maximal temperature at location r_l is indicated by ΔT. The t_r and T_d are rise time and fall time (100 ms) of temperature, respectively. The axonal membrane capacitance c_m is a function of time, so the membrane capacitor current I can be described by the following:

$$I = c_m\left(\frac{dV_n}{dt}\right) + \left(V_n + V_{rest}{}^{rest}\right)\left(\frac{dc_m}{dt}\right)$$

Herein, V_n is the intracellular potential at n^{th} segment, and $V_{rest} = -70$ mV (Fig. 2). Hence, the change of the membrane potential V_n at n^{th} segment of the unmyelinated axon is given as

$$c_m\left(\frac{dV_n}{dt}\right) + \left(V_n + V_{rest}{}^{rest}\right)\left(\frac{dc_m}{dt}\right) = \frac{d}{4\rho_i}\frac{V_{n-1} - 2V_n + V_{n+1}}{\Delta x^2} - I_{in}, \quad (8)$$

That, d is the unmyelinated axon diameter, and ρ_i is the resistivity of axo-plasma (35.5 Ωcm). I_{in} is the ionic current at n^{th} segment. Equation 7 can be solved to simulate axonal excitation by a rapid increase in local temperature. This equation was solved by the Runge-Kutta method. The details of this solution were presented in a previous study [2].

Experimental setup

To demonstrate the accuracy of analytic method, we measure the increased temperature of a phantom similar to neural tissue during INS. As depicted in Fig. 1, the temperature of the sample induced by a pulsed laser is measured by a Cu-Cons thermocouple, and the measured data are sent to a PC by a DAQ card. Here, we simulated neural tissue by distilled water. Because 70–80% of neural tissue is water, it can approximately mimic neural tissues (the absorption coefficient and thermal diffusivity of this phantom at wavelength 1450 nm (1550) is approximately 26 cm^{-1} (9.6) and $1.5 \times 10^{-7} m^2/s$ which are similar to neural tissue) [13, 18, 22]. In addition, as previous studies show, a photothermal interaction due to water absorption was the most likely mechanism behind INS.

In this study, we use a pulsed butterfly laser module at wavelength 1450 and 1550 nm that their energy and pulse duration can be adjusted up to 10 mJ per pulse and 20 ms, respectively. The laser pulse is delivered to sample via a 200-μm multimode optical fiber (NA = 0.22).

To study the feasibility of optical pacing, during open-heart rat surgery, the laser light delivered by an optical fiber to rat heart and the heartbeat are measured by ECG (Fig. 3). A miniature thermometer is used to record temperature of heart. This experimental study (including animal study) was approved by the ethic committee of Rajaie Cardiovascular Medical and Research Center, Iran.

Results

In this section, we apply MHHA model to study axonal excitation during INS. This model predicts that a rapid increase in

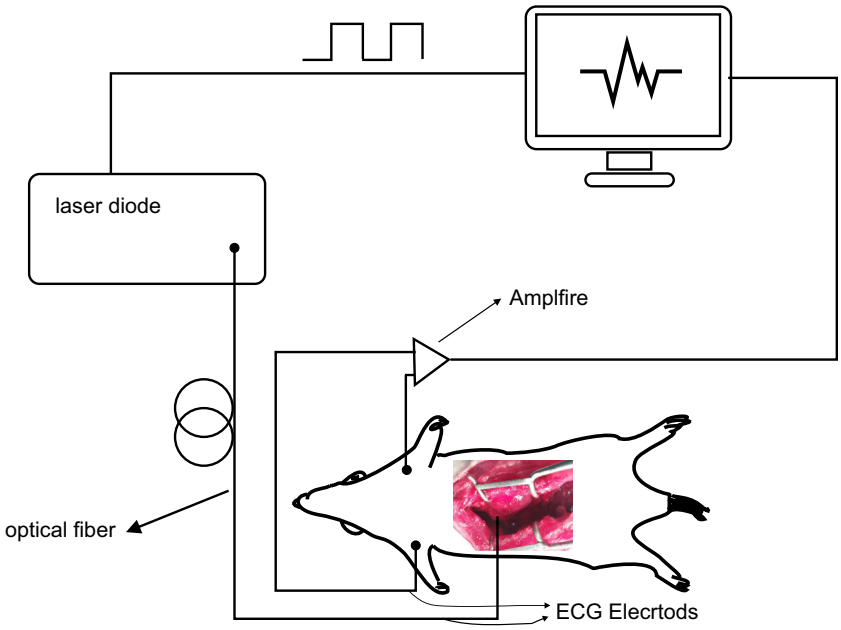

Fig. 3 Schematic of experimental set up to optical pacing. Pulsed laser light ($\lambda = 1450$ nm) is delivered to atrium; close to SA node via a 200-μm optical fiber (NA = 0.22). ECG electrodes are attached to rat, and the heartbeat is simultaneously monitored

local temperature produces an increase in membrane capacitance, which results in inward membrane current across the membrane capacitance strong enough to depolarize the membrane and generate an action potential [2]. Therefore, the first step in our analysis is to study deposited thermal energy in nervous tissues induced by a laser pulse train. As depicted in Fig. 1, the laser light is delivered to tissue via a multimode fiber optic. The most part of laser light is deposited in biological tissue, which causes a rapid increase in local temperature, and this local deposited energy diffuses into biological tissue that can be studied by Eq. (4). Therefore, the ability of the presented analytical method to simulate temporal and spatial changes in the maximal temperature during INS is evaluated. First, we simulate the spatial and temporal temperature into phantom using our analytical method. The temporal changes in temperature at sites 400, 300, 200, and 100 μm laterally displaced from the center of the laser beam are shown in Fig. 4. One can see that the maximum of temperature intensively decreases for farther points.

In the following, we evaluate the abilities and accuracy of this presented method to simulate thermal diffusion by experimental data. The effect of energy and repetition rate of laser pulse on thermal diffusion in phantom is studied (see Figs. 5, 6, and 7). The calculated increases in temperature for different

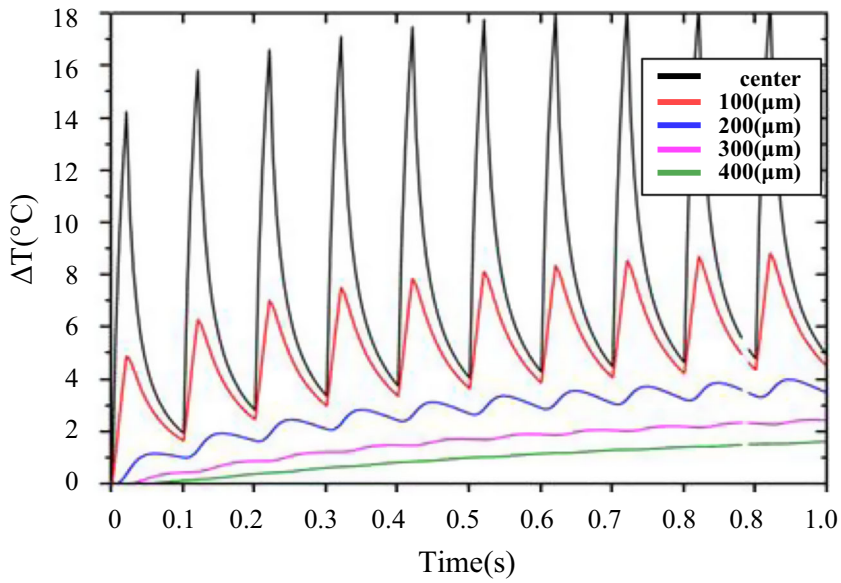

Fig. 4 Temporal changes in temperature (neural phantom) at sites 400, 300, 200, and 100 μm laterally displaced from the center of the optical fiber (NA = 0.39) for pulsed laser ($\lambda = 1550$ nm), pulse width 20 ms, repetition rate 10 Hz, and energy density 5.2 J/cm^2

energies are depicted in Fig. 5a, while the measured ΔT at 200 and 400 μm from the optical fiber core are shown in Fig. 5b, c.

The calculated variation of maximal temperature at different depths is illustrated in Fig. 6a, and b, c shows the measured temperature at depth of 100, 200, and 400 μm (due to the tip size of thermocouple, the minimal lateral displacement of the thermocouple to fiber core is approximately 200 μm). The effects of pulse repetition rate on ΔT are depicted in Fig. 7.

Based on MHHA model, a rapid increase in temperature produces a change in membrane capacitance. Hence, the variation of maximal temperature predicted by analytical method can be applied to simulate generation of action potentials. To simulate generation of action potentials during INS, Eq. (8) can be solved using Rung-Kutta with a time step of 1 μs. The MHHA model successfully simulated the generation and propagation of an action potential induced by local temperature during INS, and the simulated results show that a train of laser pulse ($\tau = 20$ ms, E = 6 J/cm^2, f = 10 Hz) at wavelength 1550 nm can raise local temperature by $\Delta T = 8^{\circ}$C, and this ΔT can produce an action potential (see Fig. 8a). This ΔT can increase the membrane capacitance from 1.0 to 1.31 μF/cm^2 (Fig. 8b). This variation results in a peak current about 120 μA/cm^2 across the membrane capacitor (see Fig. 8c).

The results also show that a minimal increase in local temperature, ΔT_0, is required to excite the axon and generate an action potential. This threshold increased temperature depends on the global axon temperature. The results show that "threshold increased temperature," ΔT_0, decrease with an increase in global axon temperature. Figure 9 depicts the effect of global axon temperature on the minimum increased temperature required to generate action potentials. In addition, the presented results in Fig. 9 indicate that rise time τ_r is a key parameter to determine the minimal temperature required for generation an action potential. Moreover, as can be seen from Eq. (8), the unmyelinated axon diameter influences on ΔT_0 that its effects are depicted in Fig. 10.

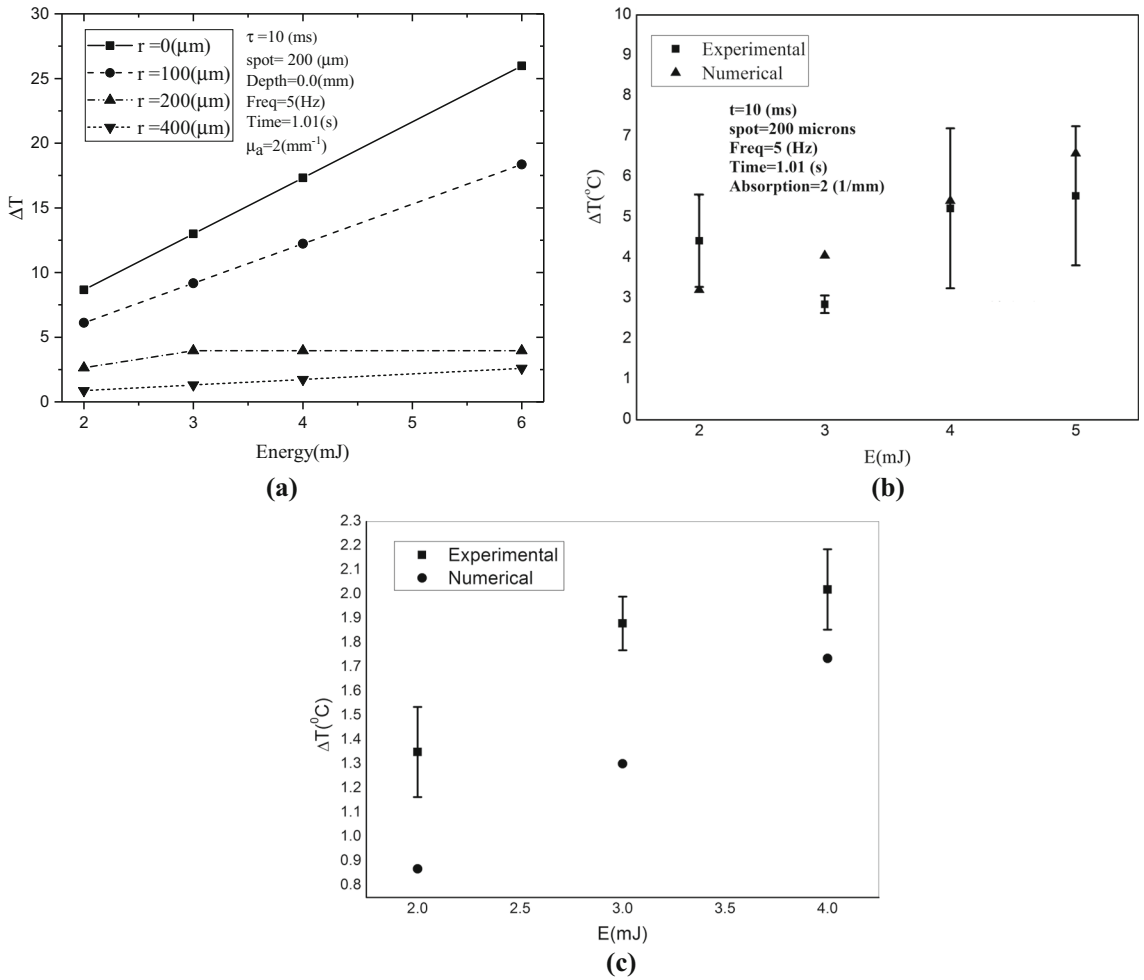

Fig. 5 The maximum calculated increase in temperature at different sites 400, 300, 200 and, 100 μm laterally displaced from the center of optical fiber. The wavelength is 1550 nm, pulse duration 10 ms, repetition rate 5 Hz. The absorption coefficient is 2 mm^{-1} and the laser spot size is 200 μm (**a**). The comparison between measured increased temperature and those obtained by analytic method (depicted in Fig. 5a) at sites 200 μm (**b**) and 400 μm (**c**) from optical fiber

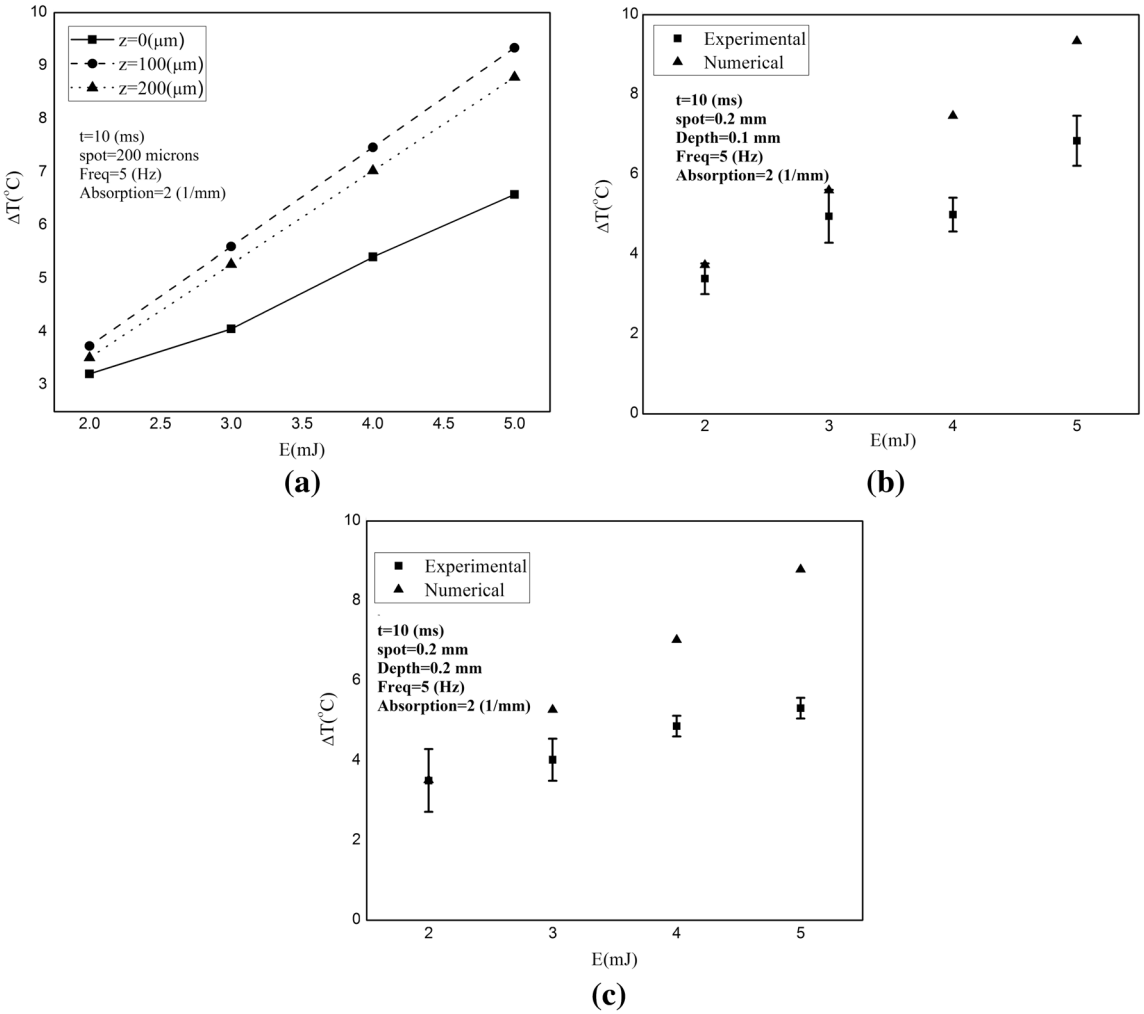

Fig. 6 Maximum increase in temperature at different depth. Calculated increased temperature at depth of 100 and 200 μm by analytic method, at time 1.02 s (**a**). The absorption coefficient is 2 mm^{-1}. A pulse laser (λ = 1550nm) with spot size 200 μm, pulse duration 10 ms, and repetition rate 5 Hz is delivered by optical fiber (NA = 0.22, diameter 200 μm). The comparison between measured date and calculated results (depicted in Fig. 6a) at depth 200 μm (**b**) and 400 μm (**c**)

The above results illustrate that the MHHA model can be applied to determine the minimal required energy density of pulse laser for generating action potentials in neural tissues. We use this model to estimate laser light parameters to perform optical pacing an adult rat.

Our model predicts that by taking into account the diameter size of cardiac neural cells (approximately 30 μm, and see Fig. 10 for global axon temperature of 25 °C) [23], we require threshold temperature larger than 5 °C. To achieve this temperature increase, the laser energy density (λ = 1450 nm) smaller than 6 J/cm^2, repetition rate larger than 3 Hz, and pulse width 18 ms can be applied for optical pacing an adult rat. During open-heart rat surgery, the laser light is delivered to the rat heart via a 200-μm multimode optical fiber (NA = 0.22). We deliver laser (λ = 1450 nm) to rat atrium, close to sinoatrial node (SA node). We increase the laser energy density to see when capture is achieved (with pulse width 18 ms and repetition rate 3.8 Hz). A 1:1 capture at energy density around 5 J/cm^2 was seen that increases heartbeat from 160 BPM to 220 BPM. We tested this capture on two rats. Successful optical pacing was established by obtaining pacing capture, stopping, and then recapturing as well as by varying the laser energy. To demonstrate that the pulse laser was pacing the heart by exciting neural cells at SA node, laser light was delivered to the other sites on the heart, but the capturing is weakly achieved for one or two beats.

Discussion

This study is aimed to investigate how an action potential is generated during INS using a train infrared laser. Our hypothesis is that required threshold values of laser light parameters to generate and propagate an action potential can be estimated using both photothermal mechanism and MHHA model. We

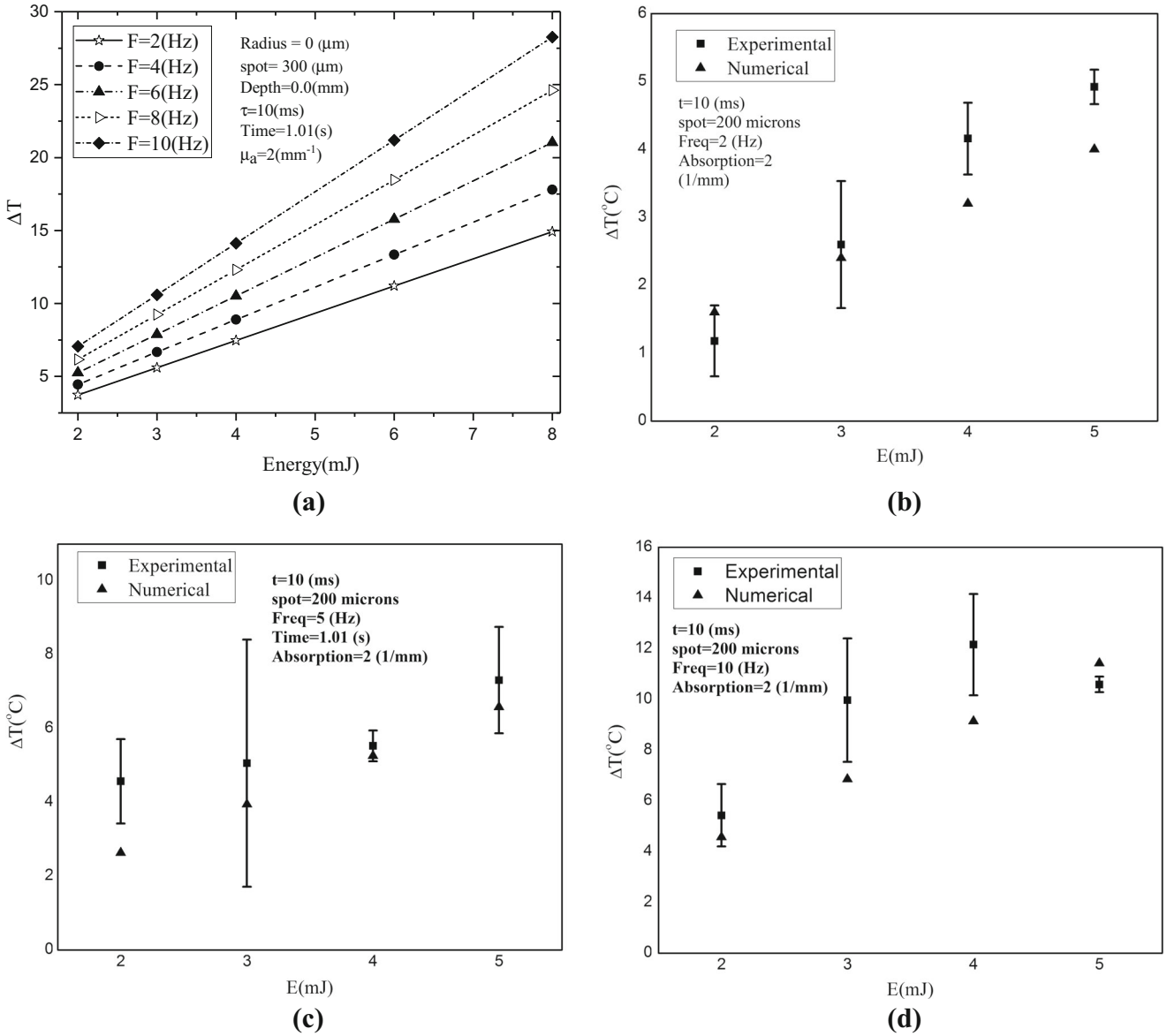

Fig. 7 Influence of repetition rate on increase in temperature as a function of energy. Calculated results by analytic method at repetition rate 2–10 Hz for energies between 2 and 8 mJ (**a**). Measured results for repletion rate 2 Hz (**b**), 5 Hz (**c**), and 10 Hz (**d**). The absorption coefficient is 2 mm^{-1}. A pulse laser ($\lambda = 1550$nm) with spot size 200 μm and pulse duration 10 ms is directed to the sample by a 200-μm optical fiber (NA = 0.22)

apply MHHA model to simulate the relation between variation of temperature and membrane depolarization.

First, we estimate the temporal and spatial variation of temperature induced by infrared lasers at wavelength 1450 and 1550 nm. Figure 4 depicts the heat diffusion for laser light (lambda = 1550 nm), pulse width 20 ms, repetition rate 10 Hz, and energy density 5.25 J/cm^2. The graphs in Fig. 4 show that the stimulation is likely to be localized to the region exposed to the laser irradiation [17]. After the first four peaks, the maximum of temperature slowly reaches to a stable value which is similar to those results presented in previous studies [10, 13]. Liljemalm et al. numerically studied heating during INS inside cortical nerve using finite element method (FEM) [10]. They stimulated cortical neurons in culture by a 500-mW (pulse width 20 ms) pulsed diode laser ($\lambda = 1550$ nm) launched into a 200-μm multimode optical fiber with a numerical aperture of 0.39, and the radiant exposure is 5.2 J/cm^2. We compare the peak temperatures at different radial points from the center of optical fiber with those numerical results presented in previous study by Liljemalm et al. (see Table 1). These analytic results are correlated with numerical results with a Pearson correlation of 0.989 ($p < 0.05$). In addition, we compare these results with experimental results presented by Bec et al. [19]. They measured the peak temperature during laser ($\lambda = 1535$ nm) irradiation of vestibular ganglion neurons (VGNs) cultured from rats and retina ganglion neurons (RGNs) isolated from C57BL/6J mice. The measured value of peak temperature for pulse duration of 20 ms is 36.0 ±

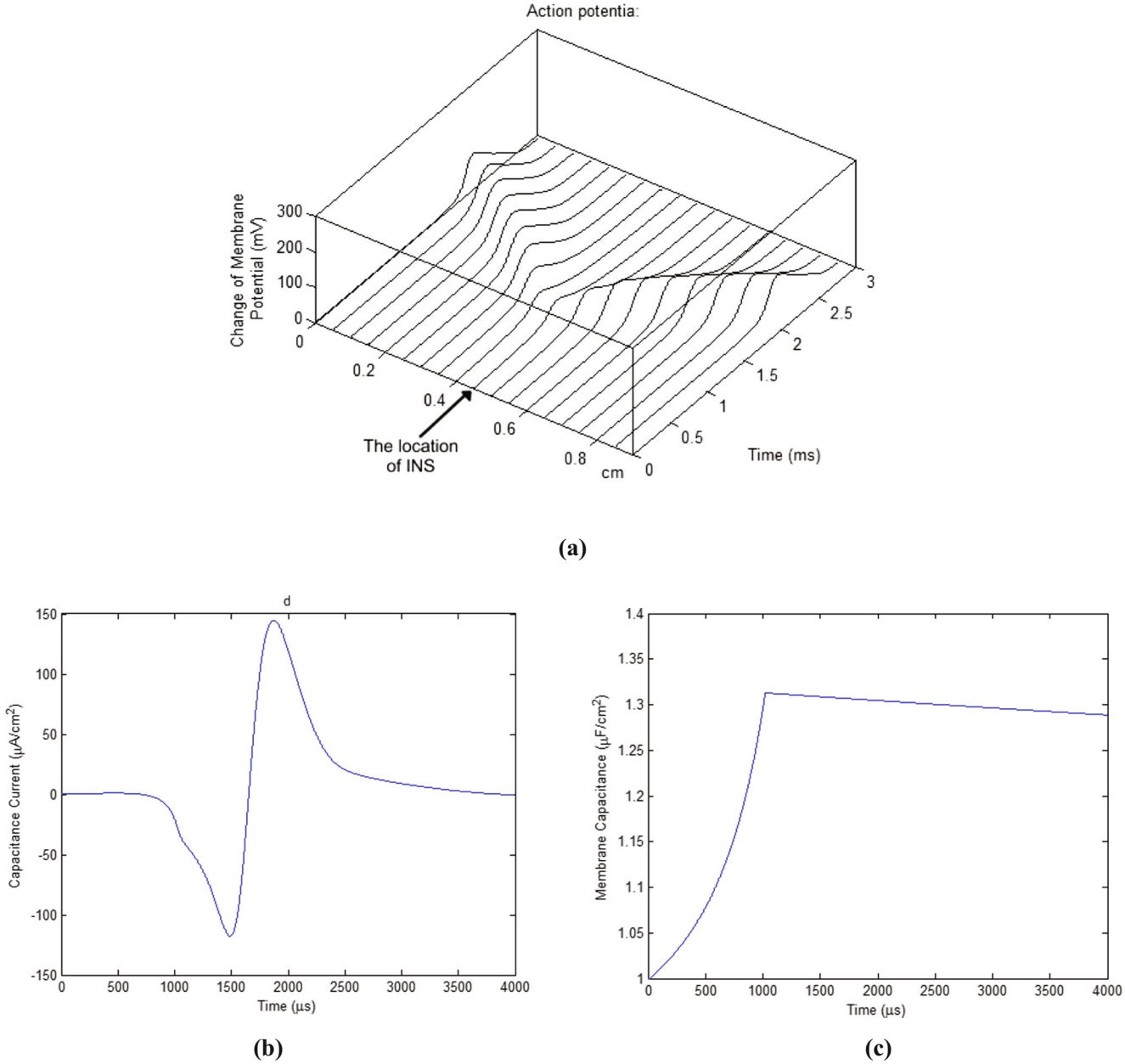

Fig. 8 Action potential induced by INS and variation of plasma membrane capacitance. Top graph shows the generation of the action potential induced by a rapid increase in the local temperature at the 0.45 cm location along the axon. One can see that this action potential propagates in both directions (**a**). The variation of membrane capacitance (**b**) and generated current across membrane capacitor (**c**) are illustrated. The laser ($\lambda = 1550$ nm) is directed to the center of axon with energy of 6 mJ, repetition rate 10 Hz, pulse duration 20 ms by a 200-μm multimode optical fiber (NA = 0.22), the diameter of axon is assumed to be 2 μm

4.0°C, that is comparable to a peak temperature of 37.0°C obtained by our method.

Then, we experimentally study the effects of variation of laser energy and repetition frequency of pulsed laser on maximum increase in temperature at different depth (see Figs. 5, 6, and 7). Experimental results show that the maximum increase in temperature depends on energy, pulse duration, and repetition rate of laser light. One can see in Fig. 7 an increase in repetition rate raises the temperature, which can be related to thermal build-up. This build-up seen in Fig. 4 will begin to occur at repetition rate larger than 4 Hz [13, 19]. The presented results indicate that the analytical method can be used to predict temporal and spatial temperature distribution in nervous tissue phantom. Therefore, we can use this method to estimate temporal variation of temperature during INS.

As mentioned in "The MHHA model," the temporal changes of temperature can depolarize neuronal membranes and generate an action potential. The required temperature

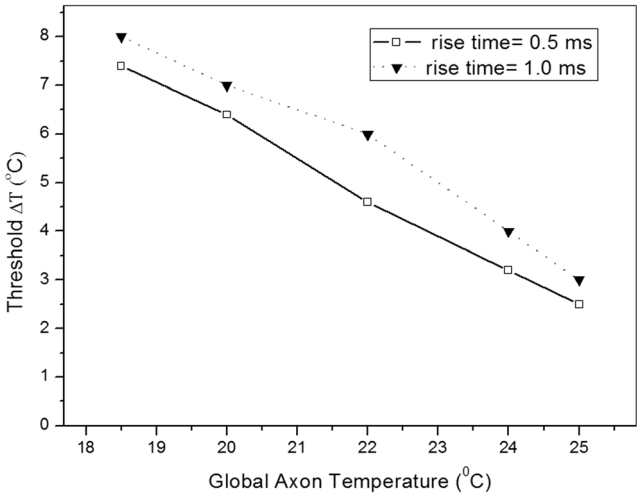

Fig. 9 Influence of global axon temperature on threshold temperature for different temperature rise times 1.0 and 0.5 ms. The diameter of axon is assumed to be 2 μm

changes to generate an action potential can be assessed using MHHA model. The graphs in Fig. 8 show that infrared laser (lambda = 1550 nm) with energy of 6 mJ, repetition rate of 10 Hz, and pulse duration 10 ms can generate and propagate an action potential inside a typical rat axon. These results depict that the combination of heat diffusion equation and MHHA model helps us to estimate the required value of laser light parameters to generate an action potential inside the heart of an adult rat. We estimate that the laser energy density (λ = 1450 nm) smaller than 6 J/cm^2, repetition rate larger than 3 Hz, and pulse width 18 ms can be applied to optical pacing an adult rat. We see that around 5 J/cm^2, the heartbeat of adult rat increases from 160 BPM to 220 BPM. Next, the heart is illuminated by a pulsed laser at λ = 1550 nm, but we could not stimulate the rat heart. The absorption coefficient of neural

Table 1 The comparison between our results (analytical method) and results obtained by FEM (presented in ref. [10]). The stable maximal temperature increase $\Delta T(^oC)$ of stimulation at sites 400, 300, 200, and 100 μm laterally displaced from the center of the laser beam. A train pulse laser @ 1550 nm with power 300 mW, repetition rate 10 Hz, pulse length 20 ms is delivered to phantom via an optical fiber (200 μm, NA = 0.39)

Radial distance	Analytic	Numerical (FEM)
At center	16.0	19.5
100 μm	9.0	8.0
200 μm	3.5	2.6
300 μm	2.0	1.4
400 μm	1.0	0.8

cells at λ = 1450 nm is approximately three times larger than λ = 1550 nm. Therefore, at this wavelength, we need more laser energy to achieve threshold increased temperature ΔT_0, which causes burns on the rat heart.

In fact, this animal study confirms the accuracy of our estimations for generating and propagating action potentials during INS. It is important to note that we could perform optical pacing in situ. Jenkins et al., in 2013, evaluated the feasibility of optical pacing an adult rabbit heart using a pulsed laser (1870 nm) with repetition rate 2.5 Hz, pulse width 8 ms, and energy density 6.3 J/cm^2. In their study, the heart was excised from a euthanized rabbit before cannulating and perfusing the heart on a modified Langendorff apparatus [9, 24].

Conclusion

The heating of nervous tissue during infrared neural stimulation was studied by heat diffusion equation. By applying an

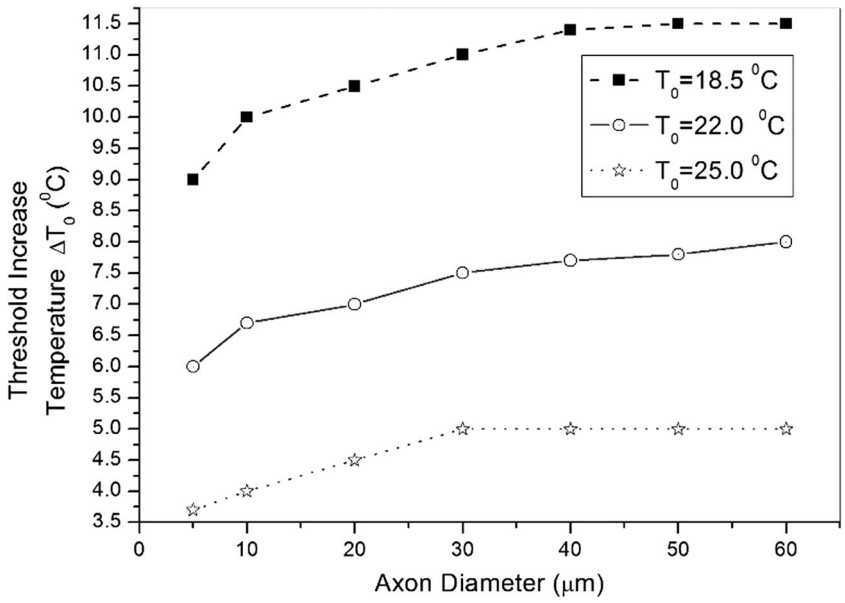

Fig. 10 The threshold increased temperature required to generate action potential as a function of axon diameter for different global axon temperatures

appropriate Green function, temporal-spatial heat distribution is determined. The accuracy of these results was verified by numerical results (FEM) and experimental data. Results indicated that the peak temperature and general temperature distributions in tissue can be controlled by laser parameters that can be useful for device safety. Furthermore, the influence of temporal evolution of temperature on membrane capacitance was simulated by MHHA model. The peak temperature required for generating an action potential in a neural tissue (depicted in Fig. 2) can be estimated by MHHA model. The peak temperature depends on axon diameter and laser parameters. Hence, we can predict the threshold value of laser parameters to trigger an action potential. The precision of predicted parameters was verified during a rat open-heart surgery for optical pacing. The optical pacing was captured by a train infrared laser pulse ($\lambda = 1450$ nm) with repetition rate 3.8 Hz, pulse duration 18 ms, and energy density 5 J/cm^2.

Therefore, the presented method can be used to estimate minimum required laser light parameters to generate an action potential, and it can provide an insight to how the temperature changes lead to neural stimulation during INS. Further in the future, the ability of this approach to infrared neural control close to SA node can be studied.

Acknowledgments Also, we would like very thank from Dr. Amir Darbandi-Azar, manager of experimental laboratory at Rajaie Cardiovascular Medical and Research Center, for helping us in animal model surgery.

Funding information This study has been supported by grant number D/1687/600 from Shahid Beheshti University.

Compliance with ethical standards

This experimental study (including animal study) was approved by the ethic committee of Rajaie Cardiovascular Medical and Research Center, Iran.

Conflict of interest The authors declare that they have no conflict of interest.

References

1. Wang J, Tian L, Lu J, Xia M, Wei Y (2016) Effect of shorter pulse duration in cochlear neural activation with an 810-nm near-infrared laser. Lasers Med Sci 32:389–396. https://doi.org/10.1007/s10103-016-2129-y
2. Fribance S, Wang J, Roppolo JR, de Groat WC, Tai C (2016) Axonal model for temperature stimulation. J Comput Neurosci 41:185–192. https://doi.org/10.1007/s10827-016-0612-x
3. Peterson EJ, Tyler DJ (2013) Motor neuron activation in peripheral nerves using infrared neural stimulation. J Neural Eng 11:016001
4. Zhao K, Tan X, Young H, Richter CP (2016) Stimulation of neurons with infrared radiation. Biomedical optics in otorhinolaryngology. Springer, New York, pp 253–284
5. Tian L, Wang J, Wei Y, Lu J, Xu A, Xia M (2017) Short-wavelength infrared laser activates the auditory neurons: comparing the effect of 980 vs. 810 nm wavelength. Lasers Med Sci 32:357–362. https://doi.org/10.1007/s10103-016-2123-4
6. Cayce JM, Friedman RM, Chen G, Jansen ED, Mahadevan-Jansen A, Roe AW (2014) Infrared neural stimulation of primary visual cortex in non-human primates. NeuroImage 84:181–190. https://doi.org/10.1016/j.neuroimage.2013.08.040
7. Wang J, Xia M, Lu J, Li C, Tian X, Tian L (2015) Performance analysis of the beam shaping method on optical auditory neural stimulation in vivo. Lasers Med Sci 30:1533–1540. https://doi.org/10.1007/s10103-015-1763-0
8. Izzo AD, Walsh JT, Jansen ED, Bendett M, Webb J, Ralph H, Richter CP (2007) Optical parameter variability in laser nerve stimulation: a study of pulse duration, repetition rate, and wavelength. IEEE Trans Biomed Eng 54:1108–1114. https://doi.org/10.1109/TBME.2007.892925
9. Jenkins MW, Wang YT, Doughman YQ, Watanabe M, Cheng Y, Rollins AM (2013) Optical pacing of the adult rabbit heart. Biomed Opt Express 4:1626–1635. https://doi.org/10.1364/BOE.4.001626
10. Liljemalm R, Nyberg T, von Holst H (2013) Heating during infrared neural stimulation. Lasers Surg Med 45:469–481. https://doi.org/10.1002/lsm.22158
11. Shapiro MG, Homma K, Villarreal S, Richter CP, Bezanilla F (2012) Infrared light excites cells by changing their electrical capacitance. Nat Commun 3:736. https://doi.org/10.1038/ncomms1742
12. Norton BJ, Bowler MA, Wells JD, Keller MD (2013) Analytical approaches for determining heat distributions and thermal criteria for infrared neural stimulation. J Biomed Opt 18:098001. https://doi.org/10.1117/1.JBO.18.9.098001
13. Wells J, Kao C, Konrad P, Milner T, Kim J, Mahadevan-Jansen A, Jansen ED (2007) Biophysical mechanisms of transient optical stimulation of peripheral nerve. Biophys J 93:2567–2580. https://doi.org/10.1529/biophysj.107.104786
14. Duke AR, Jenkins MW, Lu H, McManus JM, Chiel HJ, Jansen ED (2013) Transient and selective suppression of neural activity with infrared light. Sci Rep 3:2600. https://doi.org/10.1038/srep02600
15. Thompson AC, Wade SA, Pawsey NC, Stoddart PR (2013) Infrared neural stimulation: influence of stimulation site spacing and repetition rates on heating. IEEE Trans Biomed Eng 60:3534–3541. https://doi.org/10.1109/TBME.2013.2272796
16. Duke AR, Cayce JM, Malphrus JD, Konrad P, Mahadevan-Jansen A, Jansen ED (2009) Combined optical and electrical stimulation of neural tissue in vivo. J Biomed Opt 14:060501. https://doi.org/10.1117/1.3257230
17. Thompson AC, Wade SA, Cadusch PJ, Brown WG, Stoddart PR (2013) Modeling of the temporal effects of heating during infrared neural stimulation. J Biomed Opt 18:035004. https://doi.org/10.1117/1.JBO.18.3.035004
18. Thompson AC, Wade SA, Brown WG, Stoddart PR (2012) Modeling of light absorption in tissue during infrared neural stimulation. J Biomed Opt 17:075002. https://doi.org/10.1117/1.JBO.17.7.075002
19. Bec JM, Albert ES, Marc I, Desmadryl G, Travo C, Muller A, Chabbert C, Bardin F, Dumas M (2012) Characteristics of laser stimulation by near infrared pulses of retinal and vestibular primary neurons. Lasers Surg Med 44:736–745. https://doi.org/10.1002/lsm.22078
20. Welch AJ, Van Gemert MJC (2011) Optical-thermal response of laser-irradiated tissue. Springer, Berlin
21. Niemz M (2002) Laser-tissue interaction: fundamentals and applications. Springer-Verlag, Berlin

22. Irvine WM, Pollack JB (1968) Infrared optical properties of water and ice spheres. Icarus 8:324–360. https://doi.org/10.1016/0019-1035(68)90083-3
23. Pauziene N, Pauza DH, Stropus R (2000) Morphology of human intracardiac nerves: an electron microscope study. J Anat 197:437–459. https://doi.org/10.1046/j.1469-7580.2000.19730437.x
24. Wang YT, Rollins AM, Jenkins MW (2016) Infrared inhibition of embryonic hearts. J Biomed Opt 21:060505. https://doi.org/10.1117/1.JBO.21.6.060505